Am. J. Hum. Genet. 69:516–527, 2001

Molecular Characterization and Gene Content of Breakpoint Boundaries in Patients with Neurofibromatosis Type 1 with 17q11.2 Microdeletions

Dieter E. Jenne,[1] Sigrid Tinschert,[2] Heike Reimann,[1] Wolfgang Lasinger,[1] Gundula Thiel,[2] Horst Hameister,[3] and Hildegard Kehrer-Sawatzki[3]

[1]Max-Planck-Institute of Neurobiology, Department of Neuroimmunology, Martinsried, Germany; [2]Institute of Medical Genetics, Charité, Humboldt-University, Berlin; and [3]Department of Human Genetics, University of Ulm, Ulm, Germany

Homologous recombination between poorly characterized regions flanking the NF1 locus causes the constitutional loss of ~1.5 Mb from 17q11.2 covering ⩾11 genes in 5%–20% of patients with neurofibromatosis type 1 (NF1). To elucidate the extent of microheterogeneity at the deletion boundaries, we used single-copy DNA fragments from the extreme ends of the deleted segment to perform FISH on metaphase chromosomes from eight patients with NF1 who had large deletions. In six patients, these probes were deleted, suggesting that breakage and fusions occurred within the adjacent highly homologous sequences. Reexamination of the deleted region revealed two novel functional genes FLJ12735 (AK022797) and KIAA0653-related (WI-12393 and AJ314647), the latter of which is located closest to the distal boundary and is partially duplicated. We defined the complete reading frames for these genes and two expressed-sequence tag (EST) clusters that were reported elsewhere and are associated with the markers SHGC-2390 and WI-9521. Hybrid cell lines carrying only the deleted chromosome 17 were generated from two patients and used to identify the fusion sequences by junction-specific PCRs. The proximal breakpoints were found between positions 125279 and 125479 in one patient and within 4 kb of position 143000 on BAC R-271K11 (AC005562) in three patients, and the distal breakpoints were found at the precise homologous position on R-640N20 (AC023278). The interstitial 17q11.2 microdeletion arises from unequal crossover between two highly homologous WI-12393-derived 60-kb duplicons separated by ~1.5 Mb. Since patients with the NF1 large-deletion syndrome have a significantly increased risk of neurofibroma development and mental retardation, hemizygosity for genes from the deleted region around the neurofibromin locus (CYTOR4, FLJ12735, FLJ22729, HSA272195 (centaurin-α2), NF1, OMGP, EVI2A, EVI2B, WI-9521, HSA272196, HCA66, KIAA0160, and WI-12393) may contribute to the severe phenotype of these patients.

Introduction

Neurofibromatosis type 1 (NF1 [MIM 162200]) is a common autosomal dominant disorder characterized by the development of neurofibromas, cafe-au-lait spots, and Lisch nodules and by an increased risk of malignancy, in particular, optic gliomas, neurofibrosarcomas, and childhood myeloid leukemia (reviewed in Huson 1994). Most of the germline mutations identified in patients with NF1 so far are intragenic mutations of the NF1 gene, which cause truncation or loss of the encoded protein (Ars et al. 2000; Fahsold et al. 2000; Messiaen et al. 2000).

Haploinsufficiency for neurofibromin, the NF1 gene product, is suggested as the molecular basis of the disease. Inactivation of the remaining wild-type allele has been observed in benign and malignant tumors in patients with NF1, indicating that tumor development is most likely triggered by the acquired complete loss of functional neurofibromin in somatic cells (for review, see Side and Shannon 1998).

Approximately 5%–20% of all patients with NF1 carry a heterozygous deletion and thus lack the NF1 gene (Lopez-Correa et al. 1999; Jenne et al. 2000; Dorschner et al. 2000), and ⩾11 contiguous genes from the adjacent regions (Jenne et al. 2000). Most interstitial chromosomal fusions appear to directly link two regions of high sequence similarity that occur at distances of ~400 kb proximal and 700 kb distal to the NF1 gene. Despite the worldwide progress in sequencing that occurred during the course of this project, both regions are still not fully covered by draft sequences and continuous BAC contigs. Several expressed-sequence tags (ESTs) from uncharacterized genes have been located in the duplicated regions by radiation-hybrid mapping and BAC-based PCRs (Dorschner et al. 2000). However, the exact structural organization of the repeated segments, with regard to the unambiguous location and identification of functional genes, has not been clarified.

Received May 16, 2001; accepted for publication June 28, 2001; electronically published July 20, 2001.

Address for correspondence and reprints: Dr. Hildegard Kehrer-Sawatzki, Department of Human Genetics, University of Ulm, Albert-Einstein-Allee 11, 89081 Ulm, Germany. E-mail: hildegard.kehrer-sawatzki@medizin.uni-ulm.de

© 2001 by The American Society of Human Genetics. All rights reserved.
0002-9297/2001/6903-0006$02.00

Most patients with large interstitial deletions develop a more severe clinical syndrome than do patients with NF1 who have intragenic NF1 mutations. The gene-deletion syndrome is characterized by a dysmorphic facial appearance—including coarse features, hypertelorism, ptosis, and/or a Noonan-like face—as well as severe learning disabilities, mental retardation, developmental delay, and an excessive number of neurofibromas for patient age (Kayes et al. 1992, 1994; Wu et al. 1995; Leppig et al. 1996, 1997; Riva et al. 1996; Cnossen et al. 1997; Tonsgard et al. 1997; Rasmussen et al. 1998; Upadhyaya et al. 1998; Riva et al. 2000). The characteristic clinical and developmental phenotype of patients with the 17q11.2 microdeletion syndrome may be caused by dose-sensitive genes located in the deleted interval or close to the fusion boundaries that regulate development, organization, and function of the brain and cellular differentiation.

To elucidate the molecular basis of the 17q11.2 microdeletion syndrome, we characterized the open reading frames of new functional genes associated with the markers SHGC-2390 and WI-9521, the genes for FLJ12735 (AK022797) and KIAA0160, and the marker WI-12393. The latter two genes were found to be located at the distal boundary and are implicated in partial duplications (fig. 1). We investigated the organization of the distal and proximal homology regions and identified a 60-kb duplicated subregion on BAC R-271K11, which is fused by a mechanism of homologous recombination to a distal copy of similar size in the six patients available to us. Moreover, we performed comparative FISH analyses in the great apes, using BACs that span the two subregions of homology, to elucidate whether partial duplications and local rearrangements of both genes, KIAA0160 and WI-12393, have occurred before or during hominoid evolution.

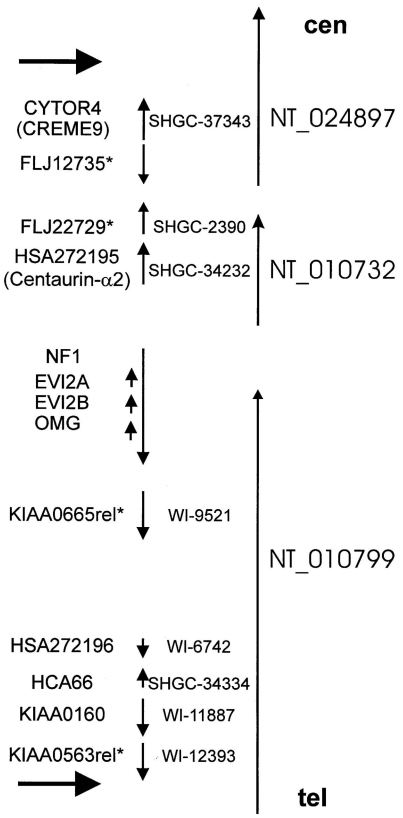

Figure 1 Contigs in 17q11.2 around the neurofibromin locus, order, and transcriptional orientation of functional genes (*vertical arrows*) and known markers (*center*) associated with these genes (*left*). Horizontal arrows (*top* and *bottom*) indicate the boundaries of the microdeleted segment that is shown in centromere (*top*) to telomere (*bottom*) orientation. Publicly available assemblies of draft segments are shown schematically (*right*), with indications of the direction (*vertical arrows*) of numbering. Conflicts between these tentative sequence paths and experimental data are reported in the present study. Asterisks indicate the four genes (AJ314645 [FLJ22729 and SHGC-2390], AJ314646 [KIAA0665rel and WI-9521], AJ314647 [KIAA0563rel and 1I-12393], and AJ314648 [FLJ12735]) whose cDNA sequences have been completed and submitted to GenBank.

Material and Methods

Subjects and Cell Lines

Peripheral blood lymphocytes were collected from patients with NF1 after informed consent was obtained. Epstein-Barr virus–transformed lymphoblastoid cell lines were established for all eight patients with NF1. Analysis that we reported elsewhere has documented an NF1 microdeletion in seven patients (Jenne et al. 2000). In the newly ascertained patient, ULM, the NF1 microdeletion was identified by FISH analysis with BAC clones, as described by Jenne et al. (2000).

Somatic cell hybrid lines were generated, to isolate the deleted chromosome 17 of two patients with NF1: ULM and COS. For this purpose, we performed polyethylene glycol–mediated fusion of lymphoblastoid cell lines with the thymidine kinase–deficient mouse cell line B82. Selection of hybrid cells was performed in medium containing hypoxanthine, aminopterin, and thymidine (Gibco BRL). After several months of growth and single-cell cloning, hybrid cell lines containing the interstitially deleted human chromosome 17 were analyzed by FISH, using BAC 542B22, and by PCR, using primer pairs for different exons of the NF1 gene, as described elsewhere (Fahsold et al. 2000). Lymphoblastoid and fibroblast cell lines from three species of great apes were kindly provided by Dr. Werner Schempp.

Clones and DNA Probes

All clones, including cDNA plasmids, P1 artificial chromosome (PAC), and bacterial artificial chromosome (BAC) clones, were purchased from Research Genetics.

Table 1

Sequences and Location of Primers Used for Fusion Point Mapping and Probe Generation

Primer Designation	Primer Sequence	Position According to AC005562[a]
DJ2066	GTGGAAGAATCAAAGCACTGTTA	112106U
DJ1738	TCTCATTTTGAGGAACACAACC	112430L
DJ1739	AACCCATCAATATCAGGAGCC	112306U
DJ2065	TTTTTCCTTTTACTGTCTGTGGTTC	112706L
DJ2050	AATTTCCAGTTCCGCCTTGG	121528U
DJ2051	CTGTCCCCCATCTCTTGAGTAGC	122240L
DJ2243	AGGGCTGGGCTGGGCTT	125263U
DJ2196	GAGGTTGCAGTGAGCCAAGACTAT	125652L
DJ2048	AGGATGGGGACCCAGTGGAAG	128029U
DJ2049	CTGGCCGTGAAAGGAAAGGAG	128476L
DJ2079	AGGCCAAGGGAGGCTGGA	139036U
DJ2080	GATGTAAAGTTCTTGGCAGGTCG	141046L
DJ2121	GAGTTGGGAAGCACAAACGTGA	141351U
DJ2122	GGGAGGGGGAGGAAGAAAAA	142341L
DJ2290	TCAACCTCCCAGGCTCCCGAA	140831L1
DJ2314	TTTGCACGTGTGACCTTCCACAG	144761L
DJ1637	TGTCATGTGGTGGGTGGTGTG	141950U
DJ2003	GCGCGAGGCCCTCTAGTAACT	142776L
DJ1754	TGACCAAGTGTCTAAAATAGGCA	171897U
DJ1755	AAATGGCTAACACTGCTGTGC	172255L
DJ1686	CAGGTTATAGGGAAGGAGGAC	WI-12393 exon 1U
DJ1863	AGCAGCGGTTAAGCAATGATG	WI-12393 exon 1L
DJ1873	GGGTACAGGGAGCCTCTGGAA	180256U
DJ1876	GTGCACCCAGCCTTGCTAAGTGCAC	188013L

[a] U = forward primer; L = backward primer.

DNA from bacteria and PCRs were purified by routine procedures (Qiagen).

FISH Analysis

BAC-DNA used as probe for FISH analysis was either labeled with biotin-16-dUTP and detected with FITC-avidin, or with digoxygenin-11-dUTP and detected with antidigoxygenin coupled with Texas-Red (Roche, Dianova), as described elsewhere (Kehrer-Sawatzki et al. 1997). Slides were counterstained with DAPI (Sigma) and examined with a Zeiss Axioskop epifluorescence microscope equipped with the ISIS image-documentation system (Metasystem).

Northern Blot Analysis

Northern blot hybridizations were performed using the Human MTN Blot (Clontech) with a ^{32}P-labeled probe WI-12393 isolated by reverse transcriptase (RT)–PCR on cDNA derived from human brain (Clontech), with the primers 5′-GCAACACTGCATGTCTG-ACTAA-3′ and 5′-CTTCATCAGGAGGCCTGTTC-3′. As a control, the blot was hybridized, after the hybridization with the WI-12393 probe, with a β-actin cDNA fragment that spanned 2 kb.

Sequence and Structure of the KIAA0160 and WI-12393 Genes

The complete cDNA sequence of the WI-12393 gene was assembled by analysis of the IMAGE clone y174c12 (GenBank accession numbers H04996 and H04995) and a combination of database searches (UniGene, the Institute for Genome Research), analysis of genomic draft sequences, comparisons with rat and mouse sequences, exon predictions, and RT-PCR analyses using human cDNAs from various tissues (Clontech). The presence and orientation of exons and the length of introns for the KIAA0160 gene were studied by long-distance PCRs with the Expand Long Template PCR System (Roche Molecular Biochemicals), using purified DNA from the BACs 307A16 and R-640N20. Other genes around the NF1 locus in the deleted interval (e.g., SHGC-2390, WI-9521, and AK022797) were assembled and completed similarly and deposited at GenBank (fig. 1).

Deletion-Junction Fragment Analysis

The deletion-junction fragments of patients COS, PFA, and WIN were amplified with phosphothioester bond–modified primers DJ2290 and DJ2314 (table 1), using the Expand Long Template PCR System (Roche Molecular Biochemicals), with 100 ng genomic DNA,

three touchdown PCR cycles, and a final annealing temperature of 68°C.

Results

FISH Analyses and Determination of the Duplicon Structure

The FISH analyses that we reported elsewhere (Jenne et al. 2000) provided strong evidence that proximal and distal breakpoints of the deletions cluster within highly homologous sequences of ~100 kb separated by a distance of 1.5 Mb in six of eight patients with NF1 (fig. 1). Conflicting physical maps published elsewhere (Dorschner et al. 2000; Riva et al. 2000) prompted us to reexamine the assembly of BAC contigs and marker locations and to reconstruct the proximal and distal breakpoint regions flanking the NF1 gene from various BACs and draft sequences. Using a cell line from a patient with NF1 in which the NF1 gene is disrupted by a balanced reciprocal translocation t(17;22) (Kehrer-Sawatzki et al. 1997), we identified a subfragment on the BAC R-271K11 amplified with primers DJ1637 and DJ1638 (table 1), which hybridized to the der(17) and the der(22) chromosome. Similar findings were obtained with the BACs R-778K9, 2309P3, and 2349P21 (see fig. 2*A*). Although the BAC 2349P21 overlaps by only 8 kb with R-271K11 (fig. 2*A*), signals on both derivative chromosomes were obtained, indicating the presence of two different duplicated regions on these two BACs (data not shown).

Two distinct segments on BACs R-271K11 and 2349P21/R-778K9 separated by ~60 kb of unique sequence (collectively termed "proximal duplicon") recur within a distance of 1.5 Mb in the opposite order (fig. 2*A* and 2*B*). The duplicated sequence on R-271K11 between position 90 kb and 150 kb covers several exons that are highly homologous to ESTs associated with the marker WI-12393 and that reoccur on the distal portion of the BAC R-640N20. The duplicated sequence on 2349P21/R-778K9 is derived from the KIAA0160 gene characterized by the STS markers stSG40099, WI-11887, and A007E42. Sequences from this gene were located on the proximal BAC R-778K9, as well as on the distal BAC R-640N20 (fig. 2*A*).

Complete Gene Structure of KIAA0160 and WI-12393 on the Distal Duplicon

We then reconstructed the functional gene copies of the KIAA0160 and the WI-12393 genes. Because the fully sequenced BAC clone 307A16 located distally to NF1 carries only the 3′ portion of the cDNA sequence (exons 5–16), the question was whether the complete gene was located on the partially sequenced BAC R-778K9. Although this clone from the proximal duplicon contains additional cDNAs (AF046059 and AK022797) telomeric to several KIAA0160 exons, exons 10–16 of the latter gene are absent. The only BAC clone that carries all 16 exons of the KIAA0160 gene is R-640N20, which partially overlaps with 307A16. We determined the distances between the first five exons on R-640N20 by PCR and showed that they were arranged in the correct order and orientation on this partially sequenced BAC (see fig. 2*A*). It became clear that clone 307A16 is internally deleted, whereas R-640N20 appears to be intact. By contrast, clone R-778K9 carries only a subregion of the KIAA0160 gene containing the first nine exons. The splice-donor site of intron 9 is mutated, and a single-base deletion within exon 5 results in a reading-frame shift, indicating that this genomic fragment on R-778K9 is most likely a nonprocessed pseudogene fragment.

An even more complex situation was found for the WI-12393 gene. The full-length cDNA sequence deposited at GenBank (AJ314647) was established by RT-PCR, using total brain cDNA and ESTs that match the sequence of BAC R-640N20. In northern blot analysis of the WI-12393 gene, two weakly expressed transcripts, of ~1.7 and 4.4 kb, were observed. The 1.7-kb WI-12393 transcript was detected in all tissues examined and could represent an alternative splice product of the WI-12393 gene. The size of this transcript, however, is also consistent with the length of a highly homologous cluster of unspliced ESTs on R-271K11 that matches the genomic sequence of R-271K11 at position 111000–112500. By contrast, the 4.4-kb mRNA transcript was identified only in skeletal muscle, kidney, and pancreas (fig. 3). It is significantly larger than the 3,017-bp cDNA sequence that we determined and submitted for the WI-12393 gene. The WI-12393 transcript is most closely related to the mRNA for KIAA0563, which has a very long (1,814 bp) 5′ untranslated region (AB011135). If the WI-12393 transcript showed a very long 5′ untranslated region similar to KIAA0563, the size of the WI-12393 transcript would be conceivable. The close relationship between the KIAA0563 and WI-12393 predicted proteins extends over the entire length of the reading frame, showing 81% identical residues.

Subfragments of the WI-12393 gene are present on both BACs, R-271K11 and R-640N20. R-271K11 carries a pseudogene-like fragment, covering exons 8–12 in the same orientation as the functional gene located on R-640N20 (fig. 2*A* and 2*B*). In addition, at the 5′ and 3′ side of this remnant, additional subfragments of WI-12393 were found; exon 8 was in opposite orientation on the 5′ side, and exons 4–5 were in opposite orientation flanking the 3′ side. In a similar, but not identical, manner, R-640N20 carries an inverted fragment covering exons 2–5 on the distal side of the functional gene. The splice-acceptor site of intron 11 on BAC R-271K11 was found to be mutated to CG, indicating that the exon

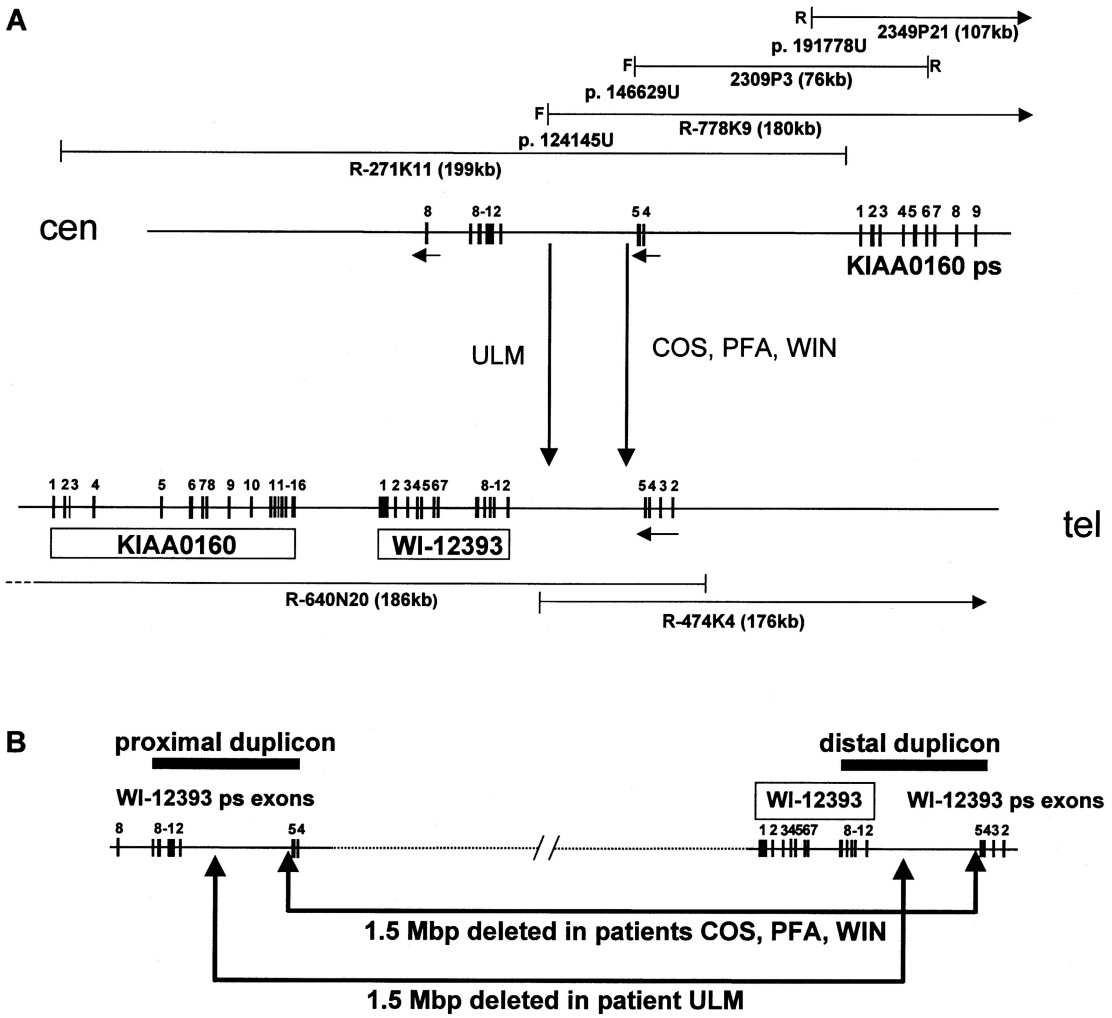

Figure 2 Structure and gene content of 17q11.2 breakpoint regions in patients with NF1 who have microdeletions. *A*, the recombination event between highly homologous sequences located 400 kb upstream (*top*) and 700 kb downstream of the NF1 gene. BAC clones characterized and used as FISH probes in this study are shown above and below the lines that represent the proximal and distal breakpoint regions. The exons of both functional genes (KIAA0160 and WI-12393), as well as the nine exons of a pseudogene fragment derived from KIAA0160 and several pseudogene exons derived from WI-12393 by duplications and local rearrangements, are shown (*black vertical bars with numbers*). The vertical long arrows indicate the fusion points that we identified in four of six patients. Clones from the RPCI-11 human male BAC library (Pieter de Jong, Roswell Park Cancer Institute) are labeled with the prefix R-, and clones without a prefix were provided by the California Institute of Technology. Clone designations are followed by the approximate size of the insert in parentheses; BAC end sequences were obtained from the Institute for Genome Research and are given by the letter F (T7 end) and R (SP6 end). *B*, Schematic representation of two highly homologous segments (*black horizontal bars labeled "proximal duplicon" and "distal duplicon"*) that are implicated in the 17q11.2 microdeletion syndrome. This scheme illustrates the complete deletion of the functional WI-12393 gene (*boxed*), together with 12 additional genes (not shown, indicated by the dotted interrupted line) in all six patients and the location and orientation of the proximal and distal WI-12393–derived ~60-kb duplicon. Homologous WI-12393 exons (WI-12393 pseudogene exons) are indicated (*thin vertical bars*). The precise breakpoint has been mapped in four patients: COS, PFA, WIN, and ULM (see fig. 5).

12 homologue of R-271K11 is not functional. Nevertheless, at least five partially spliced EST sequences (BG166747, AA836213, AI376737, BE082040, and BE081476) exactly match exons 10 and 11 from R-271K11 and terminate at the polyadenylation site 109324 on R-271K11 within intron 11. Two cDNA clones (AA910341 and AL359623) start further upstream and represent putative exons at 83469–83586 and 85913–85966 (AA910341 and AL359623). Two hypothetical exons at 123389–123480 and 138584–

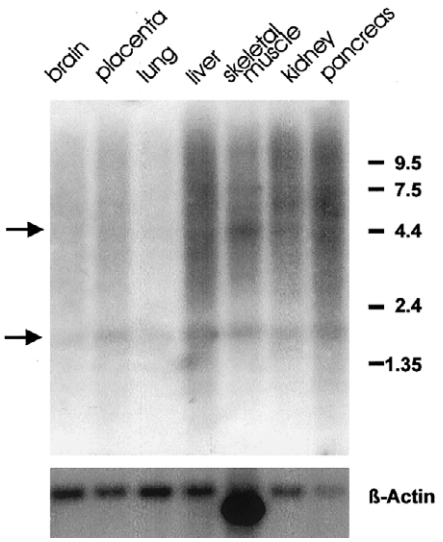

Figure 3 Northern blot analysis of WI-12393 with RNA isolated from different human tissues revealed a low expression in several adult tissues. The lower arrow indicates the 1.7-kb transcript expressed in all tissues examined; the upper arrow indicates a 4.4-kb spanning mRNA. In skeletal muscle, an additional isoform of ~7.5 kb is visible. On the right side, the positions of bands of a size marker are given in kilobases.

140722 on R-271K11 are indicated by AL359623. Certain combinations of these exons may well represent a variably spliced gene with coding potential.

Fine Mapping of Breakpoint Fusions

We first attempted to localize the deletion boundaries by using FISH with PCR-generated single-copy probes. Exon 1 of WI-12393 was a suitable probe and was shown to be deleted in all our patients. The unique region around exons 6 and 7, however, was too small for chromosomal metaphase hybridizations. The probe generated with the primer pair DJ1873/DJ1876 (ranging from position 180256 to position 188013) (table 1) was also deleted in all our patients and indicated that the entire KIAA0160 sequence of the proximal duplicon was lost. These results strongly suggest that all fusions occurred within a duplicated highly homologous stretch of 60 kb (between nucleotide position 90,000 and 150,000 on R-271K11) shared by R-271K11 and R-640N20 (fig. 2). We have not found evidence that the anticipated variability of fusions within these two segments could eliminate an additional functional gene in patients with certain deletions. We therefore conclude that the spectrum of clinical features observed in these patients is caused by the same haploinsufficiency status.

PCR-Based Identification of Breakpoint Fusions

To precisely localize the fusion sequences, we generated and selected hybrid cell lines from two patients (COS and ULM). These hybrid cell lines carry only the human chromosome 17 with the microdeletion. A series of PCR reactions were designed to amplify segments from the 60-kb duplicated region (see table 1). The sequences of these products were compared with the sequences of the proximal and distal duplicons, and they matched either the sequence of R-271K11 or the draft sequence of BAC clone R-640N20. Additional PCRs were designed to amplify the fusion segment from the DNA of our hybrid cell lines. The fusion points of patients COS and ULM were located at positions 125001–126000 and 142001–143000, respectively (numbering according to AC005562) (fig. 4). Amplification of fusion fragments from total DNA of the patient COS was achieved by selection of primers that discriminate between the proximal and distal copy as well as a third highly homologous copy of this duplicon on chromosome 19 (AC011509 and AC08569) (fig. 4). To prevent the proofreading correction of single mismatches at the 3′ end of primers by the polymerase enzyme mixture, we introduced a phosphothioester bond at the 3′ end of our primers. This primer modification resulted in a selective amplification of the fusion fragments in DNA of patient COS (DJ2290/DJ2314), whereas no products were obtained from normal DNA samples (fig. 5). To test the possibility that breakpoints are clustered within the 4-kb region covered by our PCR, we analyzed the remaining patients (PFA, KAE, WEH, and WIN) and found two additional patients (PFA and WIN) whose fusion falls at almost the same position as that of the patient COS (fig. 5).

Evolutionary History of NF1-Flanking Duplicons

To assess the evolutionary history of the repeat sequences flanking the NF1 gene region, we performed FISH analysis on metaphase chromosomes and interphase nuclei of blood lymphocytes from unaffected donors, patients with NF1 with microdeletions, and several species of great apes. We used two probes: BAC R-271K11 spanning only the WI-12393 repeat or BAC R-640N20 containing both the KIAA0160 and the WI-12393 genes, in combination with the differentially labeled single-copy BAC 542B22, which just borders BAC R-640N20 on its proximal side and carries the markers D17S2039, WI-6742, and SHGC-34334. As seen in fig. 6A, cohybridization of BAC R-640N20 with the differentially labeled BAC 542B22 to metaphase chromosomes of one patient with NF1 (ULM) reveals a strong signal of BAC R-640N20 on the normal chromosome 17 and a strongly reduced signal of this BAC

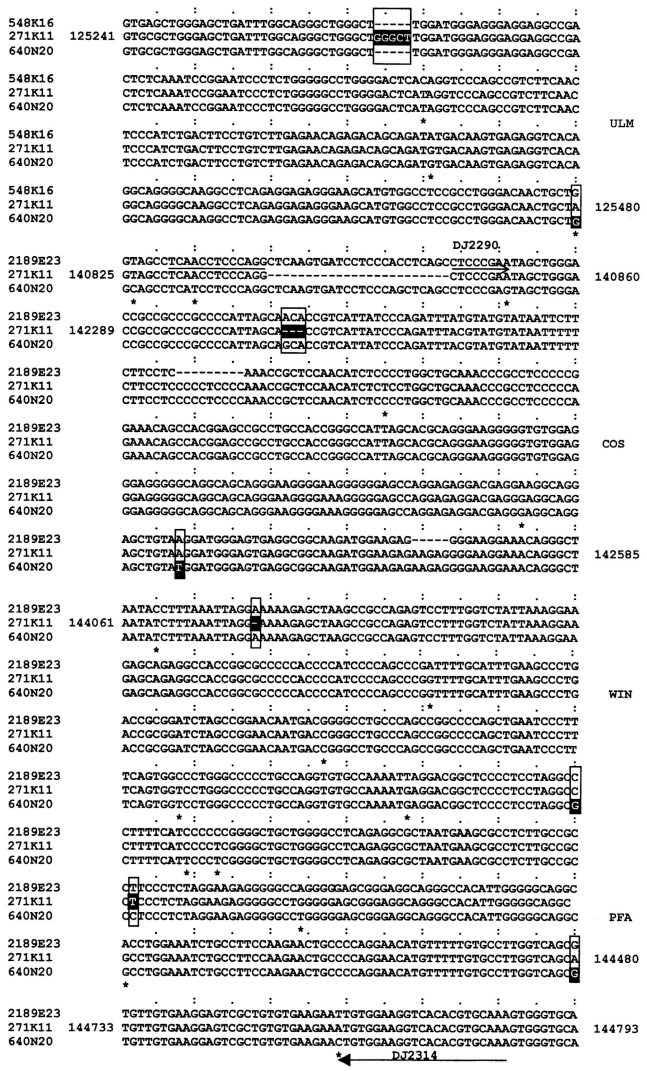

Figure 4 Alignment of three genomic sequences for the most-conserved WI-12393–derived duplicons found in 17q11.2 (BACs R-271K11 and R-640N20) and 19p13.2 (BAC 2189E23). Only those sections (125241–125480, 142289–142585, and 144061–144480) that cover breakpoint fusions and the binding sites for the primers DJ2290 and DJ2314 (140825–140860 and 144733–144793) are depicted. The locations of the forward primer, DJ2290, and the backward primer, DJ2314, which were designed to amplify fusion fragments from total DNA of patients are marked by horizontal arrows above and below the respective sequences. The nucleotides are numbered according to the completely sequenced clone R-271K11 (AC005562) at the beginning and end of each section. Every fifth and tenth nucleotide position is marked by one or two dots above the first row of the alignments. The asterisks below the aligned sequences show positions at which one or more sequences vary. The last unique nucleotide from the proximal (*middle row*) and distal (*distal row*) duplicon that border the fusion segment in the patients ULM, COS, WIN, and PFA (*right*) are shown in white on a black background; all three nucleotides at that position are boxed.

on the deleted chromosome 17. Because the deletion encompasses BAC 542B22, no signal of this BAC is observed on the chromosome 17 with the deletion. Weak signals of BAC R-640N20 are noticed in 17q21-q24, on chromosome 19p13.1 and on 3q13.3-q21. These cross-hybridizations result from more distantly related copies or pseudogene fragments of the WI-12393 gene. In 17q24, a third, but more divergent, partial copy of the WI-12393 gene is found on BAC 147L13 (AC005332). In interphase nuclei of patient ULM, only one signal of BAC 542B22 is seen flanked by two signals of BAC R-640N20 hybridizing to both duplicons, one distal and one proximal to BAC 542B22. In these nuclei, a reduced signal of BAC R-640N20 is observed, indicating the partial deletion of this BAC from one chromosome 17 homologue. On metaphase chromosomes of the chimpanzee (*Pan troglodytes*) (*PTR*), the gorilla (*Gorilla gorilla*) (*GGO*), and the orangutan (*Pongo pygmaeus*) (*PPY*), strong hybridization signals of BAC R-271K11 or R-640N20 are present in the region orthologous to human 17q11.2, and much weaker signals are present in the chromosomal region orthologous to human 17q21-24 (table 2; fig. 6*A–D*). The intensity of the hybridization signal for each of these BACs in the region orthologous to human 17q11.2 already suggests the presence of both duplicons flanking the NF1 gene region in these primates. This finding was further confirmed by the analysis of G_0/G_1 interphase nuclei. The red signal of the single-copy BAC 542B22 is flanked by the green signals of the duplicon BAC R-271K11 (fig. 6*B* and 6*C*) and R-640N20 (fig. 6*D*). In all great apes analyzed, an additional weak hybridization signal of both BACs R-

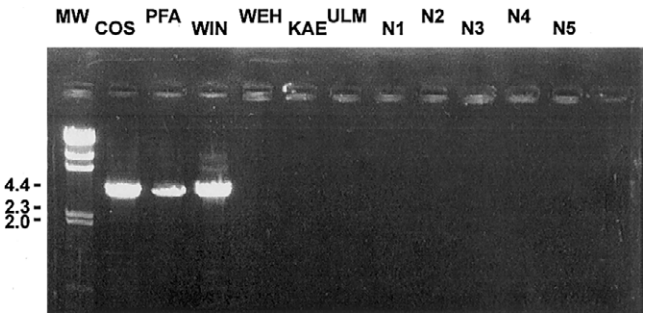

Figure 5 PCR analysis of the fusion between the proximal and distal duplicon on 17q11.2. The primers DJ2290 and DJ2314 were designed specifically to prime the proximal and distal duplicon sequence (see fig. 4). Thus, only certain patients (COS, PFA, and WIN), who had a proximal breakpoint between position 140852 and 144761 (numbering according to AC005562) and a distal breakpoint within the same homologous segment on R-640N20, show a ~4-kb amplified product that was identified by agarose gel electrophoresis. The breakpoints of patients WEH and KAE have not been identified at the sequence level. N1–N5 are DNA samples from unaffected control individuals.

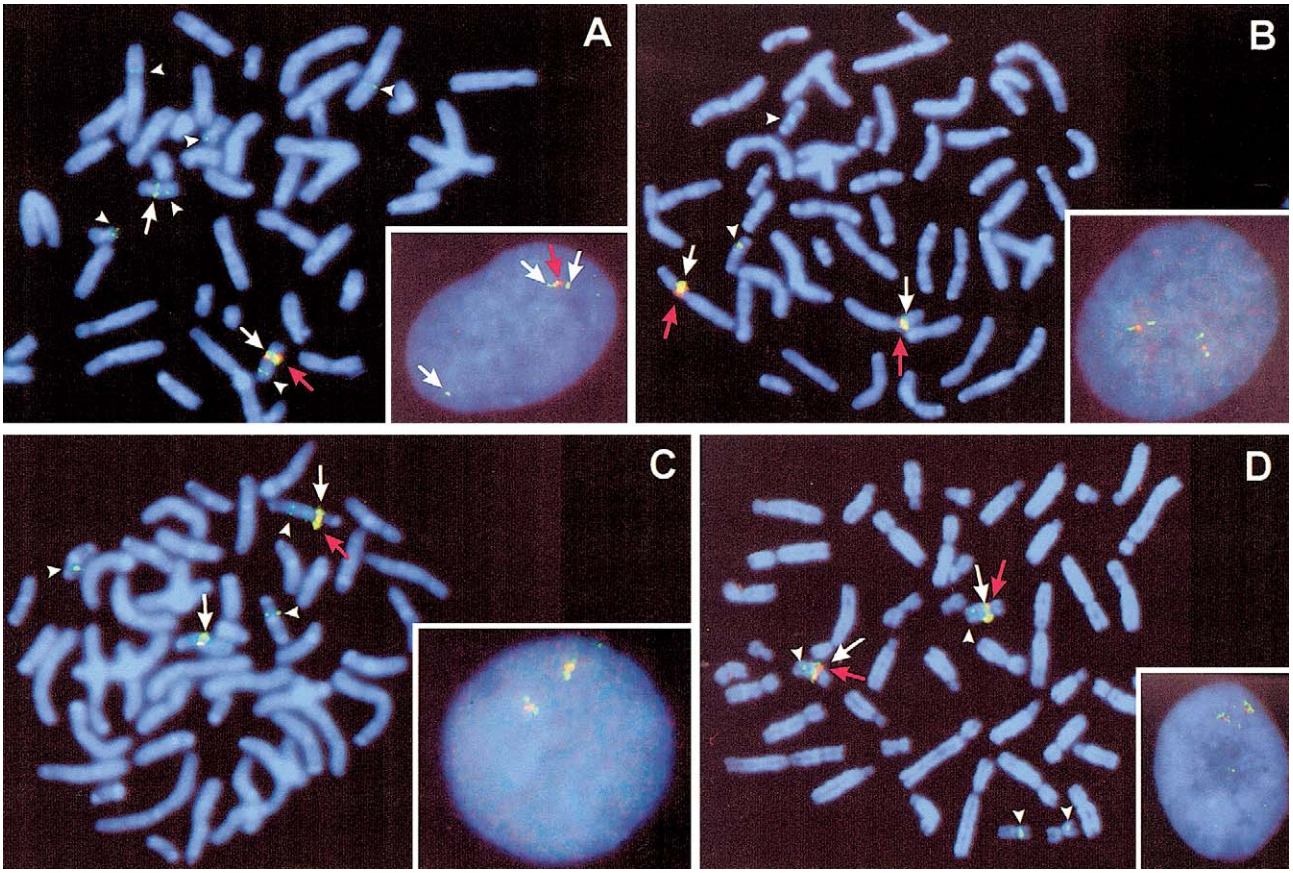

Figure 6 FISH analysis of metaphase chromosomes and interphase cells of the patient ULM, who had a 17q11.2 microdeletion, and of *GGO, PTR,* and *PPY*. The probes were BACs spanning the distal (R-640N20) or the proximal duplicon (R-271K11) (*green signals*) in combination with the differentially labeled single-copy BAC 542B22 (*red signal*) located between the duplicons. In all panels, the main hybridization signals of the duplicon BACs are indicated by white arrows, whereas the sites of weak cross-hybridization of these BACs are indicated by white arrowheads. The hybridization sites of BAC 542B22 are emphasized by red arrows. *A,* BAC R-640N20 (*green signal*) and BAC 542B22 (*red signal*) hybridized to metaphase chromosomes and an interphase nucleus of a patient (ULM) with NF1. On the normal chromosome 17, a strong signal of R-640N20 is observed, whereas on the chromosome 17 with deletions, only a reduced signal of this BAC is seen at 17q11.2 (*white arrows*). BAC 542B22 hybridizes only to the normal chromosome 17 (*red arrow*). Weak cross-hybridization signals of BAC R-640N20 are visible at 17q21-q24, 19p12-p13.1, and 3q13.3-3q21 (*white arrowheads*). *A, inset,* an interphase nucleus of patient ULM with 542B22 (*red arrow*) flanked by R-640N20 (*green signals, white arrows*). A reduced signal of R-640N20 is visible in another region of the nucleus derived from the deleted chromosome 17. *B,* Reciprocal translocation between the *GGO* chromosomes orthologous to human chromosomes 17 and 5 (*GGO* chromosomes 4 and 19). Strong signals of BAC R-271K11 (*white arrows*) and a weaker signal of the single-copy BAC 542B22 (*red arrows*) are seen at *GGO* 4p11-p12 in the region orthologous to human 17q11-q12. A weak signal of BAC R-271K11 has been observed at 4p16-17 (data not shown) and at 20p12-p13, which is orthologous to human 19p12-p13.1 (*white arrowheads*). *B, inset,* BAC R-271K11 flanking BAC 542B22 on both sites in an interphase cell. *C,* BAC R-271K11 (*white arrows, green signals*) visible at *PTR* chromosome 19p11-p12, owing to a pericentric inversion and cohybridizing there with BAC 542B22 (*red arrows*). Weak cross-hybridization signals of BAC R-271K11 are observed at *PTR* 19q14-q22 and at *PTR* 20p12-13, orthologous to human 17q21-24 and human 19p12-p13.1, respectively (*white arrowheads*). *C, inset,* an interphase cell of *PTR*, in which the single-copy BAC 542B22 (*red signal*) is flanked by BAC R-271K11 (*green signals*). *D,* BAC R-640N20 (*white arrows*) cohybridized with single-copy BAC 542B22 (*red arrow*) to metaphase chromosomes of the *PPY*. A strong hybridization signal of BAC R-640N20 and a weaker signal of BAC 542B22 are visible at *PPY* 19q11-q12, orthologous to human 17q11-q12. Additionally, weak signals of BAC R-640N20 are seen at *PPY* 19q14-q22 and at *PPY* 20p12-p13. *D, inset,* an interphase cell of PPY, in which the BAC 542B22 (*red signal*) is flanked by BAC R-640N20 (*green signals*).

271K11 and R-640N20 is visible on chromosome 20 of *PTR, GGO,* and *PPY* in the region orthologous to human 19p13.1. Cross-hybridization of these BACs in regions orthologous to human 3q13.3-q21 was not found in the great apes in this study.

Discussion

We investigated the hypothesis that recombination within highly homologous repeated sequences flanking the NF1 tumor-suppressor locus results in a 1.5-Mb in-

Table 2

Summary of FISH Results Obtained with BACs from the Duplicons and with the Single-Copy BAC 542B22 from the Distal NF1 Flanking Regions on Metaphase and Interphase Nuclei of Human (*HSA*), *PTR, GGO,* and *PPY*

BAC (GenBank Accession Number)	Sequence Content[a]	FISH Signal(s) at Chromosomal Loci[b]		
		17q11.2 (*HSA*) 19p11-12 (*PTR*) 4p11-p12 (*GGO*) 19q11-q12 (*PPY*)	17q21-q24[c] (*HSA*) 19q14-q22 (*PTR*) 4p14-p16 (*GGO*) 19q14-q22 (*PPY*)	19p13.1-p13.2[d] (*HSA*) 20p12-p13 (*PTR*) 20p12-p13 (*GGO*) 20p12-p13 (*PPY*)
R-271K11 (AC005562)	LIP12-like, AL117394, KRT17-like, KIAA0563rel ps (WI-12393)	+/+	(+)	+
2309P3	KIAA0160 ps (exons 1–6)	+/+	−	+
2349P21	KiAA0160 ps (exons 1–9), CREME9, FLJ12735	+/+	−	(+)
R-640N20 (AC023278)	KiAA0160, KIAA0563rel ps (WI-12393)	+/+	(+)	(+)
542B22 (AC004253)	HSA272196 (WI-6742), SHGC-34334 (HCA66)	+	−	−

[a] ps = pseudogene fragment.

[b] Indication of orthologous chromosomal bands, according to Yunis and Prakash (1982) and Hamerton and Klinger (1975). +/+ = double signal confirmed by analyses of G_1-interphase nuclei in cohybridization with the differentially labeled single-copy BAC 542B22; + = positive signal; (+) = weak hybridization signal on metaphase chromosomes; − = no signal.

[c] Cross-hybridization to R-147L13 (AC005332).

[d] Cross-hybridization with genomic sequences on BAC 2189E23 (AC011509) and 548K16 (AC008569).

terstitial deletion of chromosome 17 (Dorschner et al. 2000; Jenne et al. 2000). FISH analyses permitted us to locate the site of paralogous recombination within a 60-kb region and to exclude a second 20-kb repeat region covering the exons 1–9 of the KIAA0160 gene. The latter 20-kb repeat region has the same orientation and is deleted in all patients studied. Two fusion points were precisely determined using DNA from somatic cell hybrids that retain only the rearranged microdeleted chromosome 17. The fusion points fell at different sites, which are ~18 kb apart. The chromosomes of two additional patients, PFA and WIN, appear to have their breaks at the same site within the 60-kb WI-12393-derived repeat, because we were able to amplify the same fusion product from total DNA of peripheral blood cells in these patients.

During recent years, several disorders have been found to be caused by rearrangements between duplicons (reviewed by Lupski et al. 1998; Ji et al. 2000), but the breakpoints involved have been sequenced only in Charcot-Marie tooth disease type 1A (CMT1A) and hereditary neuropathy with liability to pressure palsies (HNPP) (Lopes et al. 1999), two peripheral neuropathies with different clinical and histopathological features. The CMT1A-repeats flank a 1.5-Mb region containing the dose-sensitive peripheral myelin protein 22 (PMP22) gene in 17p11.2. Misalignment of the repeat sequences leads to the duplication in patients with CMT1A, whereas the deletion of the corresponding region has been found in patients with HNPP (Boerkoel et al. 1999). The size of the rearranged genomic segment (1.5 Mb) in CMTA1/HNPP is very similar to that in the NF1 microdeletion syndrome, but there are also clear differences. The duplicons triggering 17q11.2 microdeletions have a total size of ~85 kb and are significantly larger than the CMT1A/HNPP repeats, which are 24 kb (Pentao et al. 1992; Kiyosawa et al. 1995; Reiter et al. 1997). Furthermore, the majority (~80%) of 17q11.2 microdeletions are of maternal origin and are caused by an unequal crossover between chromosome 17 homologues during meiosis (Lazaro et al. 1996; Lopez-Correa et al. 2000). In CMT1A, most of the duplications (92%) are also generated by interchromosomal crossover during meiosis but are of paternal origin. By contrast, the rearrangements in HNPP and CMT1A that have been observed in the maternal germline are caused by unequal intrachromosomal recombination (Lopes et al. 1998).

Most of the breakpoints in the CMT1A repeats occur in two segments of 557 bp and 2 kb (Reiter et al. 1998). Our observation, that the breakpoints cluster within the same 4-kb spanning fragment in three of eight patients with NF1 who have microdeletions, strongly suggests that this segment is repeatedly involved in recombination. Further studies on additional patients with NF1 who have microdeletions are needed to evaluate the presence of a recombination hot spot. The PCR that we established is a sensitive and simple procedure to specifically amplify this fusion fragment from total DNA and to identify additional patients with almost identical fusions.

An emerging feature of recombinogenic local repeats associated with such syndromes as velocardiofacial/DiGeorge, cat eye, Williams, Smith-Magenis, and Prader-Willi/Angelman is the presence of transcribed sequences within the duplicated regions, which can originate from both the functional genes and the duplicated pseudogene fragments. To identify the functional genes on

17q11.2 from which the duplicated sequences were derived, we constructed detailed physical maps for both the proximal and distal duplicon regions and compared them with the draft maps from Celera and the International Human Genome Consortium that became available after completion of our work (Lander et al. 2001; Venter et al. 2001). The maps of Celera and the International Human Genome Consortium show significant discrepancies and assembly errors in the NF1 flanking regions, which result from duplicated sequences within BAC inserts (R-640N20), instability of the cloned DNA inserts (BAC 307A16 and PAC 41C23), and inadequate computer algorithms to evaluate the quality of the automatic map assemblies. The first 77 bp of the WI-9521 cDNA are not covered by the fully sequenced PAC 41C43, nevertheless sequence homologies to the mouse genome clearly support the existence of this exon and more 5′ upstream sequences (data not shown). The KIAA0160 gene is only partially represented by the fully sequenced clone 307A16 from exons 5–16. Exons 1–4 are thus missing in the recently published human genome sequence (nt_010799). We excluded the possibility that the genomic sequence on 307A16 is only a pseudogene fragment of KIAA0160, and we showed that missing exons are found on the BAC R-640N20 in the correct orientation and transcriptional order. The presence of a highly homologous long inverted repeat on BAC R-640N20 has presumably caused false sequence extensions and BAC assemblies. The order and assembly of draft segments outlined by figure 2 are fully consistent with our FISH analyses of microdeleted chromosomes, with the translocation derivatives der(17) and der(22), and with the comparison to the draft segments of BAC R-474K4, which contains only one copy of the sequences occurring twice on R-640N20.

In the present study, we prove that homologous recombination occurs, in most cases, between two large (60-kb) homologous subfragments, both of which are derived from the WI-12393 gene by partial duplication, and we exclude the possibility of recombination between a KIAA0160 pseudogene fragment on R-778K9 and the functional KIAA0160 gene on R-640N20 (fig. 2). Because the WI-12393 duplicon borders the functional WI-12393 gene on its distal side, the latter newly identified gene is also lost, together with ⩾12 functional genes, in six of our eight patients with 17q11.2 microdeletions (fig. 1). The majority of these patients thus form a genetically homogenous group, with hemizygosity for the same set of ⩾13 genes.

In contrast to duplicon-mediated rearrangements of other chromosomal regions, constitutional microdeletions of 17q11.2 eliminate an important tumor-suppressor gene, and the somatic inactivation of the second NF1 allele is predicted to trigger the formation of tumors associated with NF1-like neurofibromas. In patients who have NF1 with 17q11.2 microdeletions, an early onset of growth and an excessive number of cutaneous neurofibromas have been observed, suggesting that a modifier gene, which has been co-deleted, favors neurofibroma development in these patients. Reduced expression levels or acquired inactivation of other hemizygous genes may additionally contribute to an accelerated growth leading to malignant transformation, because the incidence of malignant tumors of peripheral nerve sheath seems to be increased among patients who have NF1 with microdeletion (Dorschner et al. 2000). Good candidates for such modifier genes are AF046059 (CREME9) and AJ272195 (centaurin-α2). In addition, dose-sensitive genes may affect critical steps in CNS development and may thus increase the risk of mental retardation.

Interstitial rearrangements eliminating the NF1 locus by homologous recombination, using paralogous sequences as substrates, are not restricted to germ cells undergoing meiosis but can also occur somatically during mitosis, as documented in a patient with a postzygotically acquired 17q11.2 microdeletion resulting in segmental neurofibromatosis (Tinschert et al. 2000). The incidence of somatic rearrangements mediated by the same NF1 flanking duplicons is currently unknown but could be an important intermediate step that leads to malignancies in patients with NF1 (Colman et al. 1995).

Our initial speculation that the gene dose effects of additional KIAA0160 or WI-12393 copies could have played at least a transient role during recent primate evolution must be rejected. Duplicates of the WI-12393 and KIAA0160 genes are present at orthologous chromosomal loci in all hominoid species under study (fig. 6) and most likely in macaques as well (data not shown). FISH patterns in the great apes strongly suggest that amplification and dispersion of sequences orthologous to the NF1-associated flanking regions started before the divergence of the great apes (Hominoidea) ⩾8–9 million years ago (Kumar and Hedges 1998). Further studies in Old World monkeys (Cercopithecidae) and the analysis of divergence rates, however, are needed to elucidate the relationship and functional status of conserved sequences that cross-hybridize with WI-12393–derived duplicons in macaques.

Acknowledgments

D.E.J. thanks Professor H. Wekerle for his continuous interest and support of the project. This work was supported by the Sonderforschungsbereich 469 (project A5) of the

German Research Council and the European Commission (BMH-98-3865).

Electronic-Database Information

Accession numbers and URLs for data in this article are as follows:

GenBank, http://www.ncbi.nlm.nih.gov/Genbank (for IMAGE clone y174c12)
Human Genome, http://www.ncbi.nlm.nih.gov/genome/guide/human (for draft sequences of the human genome)
Institute for Genome Research, http://www.tigr.org (for draft sequences of the human genome)
Online Mendelian Inheritance in Man (OMIM), http://www.ncbi.nlm.nih.gov/Omim (for NF1 [MIM 162200])

References

Ars E, Serra E, Garcia J, Kruyer H, Gaona A, Lazaro C, Estivill X (2000) Mutations affecting mRNA splicing are the most common molecular defects in patients with neurofibromatosis type 1. Hum Mol Genet 9:237–247

Boerkoel CF, Inoue K, Reiter LT, Warner LE, Lupski JR (1999) Molecular mechanisms for CMT1A duplication and HNPP deletion. Ann N Y Acad Sci 883:22–35

Cnossen MH, van der Est MN, Breuning MH, van Asperen CJ, Breslau-Siderius EJ, van der Ploeg AT, de Goede-Bolder A, van den Ouweland AM, Halley DJ, Niermeijer MF (1997) Deletions spanning the neurofibromatosis type 1 gene: implications for genotype-phenotype correlations in neurofibromatosis type 1? Hum Mutat 9:458–464

Colman SD, Williams CA, Wallace MR (1995) Benign neurofibromas in type 1 neurofibromatosis (NF1) show somatic deletions of the NF1 gene. Nat Genet 11:90–92

Dorschner MO, Sybert VP, Weaver M, Pletcher BA, Stephens K (2000) NF1 microdeletion breakpoints are clustered at flanking repetitive sequences. Hum Mol Genet 9:35–46

Fahsold R, Hoffmeyer S, Mischung C, Gille C, Ehlers C, Kucukceylan N, Abdel-Nour M, Gewies A, Peters H, Kaufmann D, Buske A, Tinschert S, Nurnberg P (2000) Minor lesion mutational spectrum of the entire NF1 gene does not explain its high mutability but points to a functional domain upstream of the GAP-related domain. Am J Hum Genet 66: 790–818

Hamerton JL, Klinger HP (1975) Nomenclature and presumptive homologies of the chromosomes of Hominoidea In: Bergsma E (ed) Birth defects. Karger, Basel, pp 14–28

Huson SM (1994) Neurofibromatosis 1: a clinical and genetic overview. In: Huson SM, Hughes RAC (eds), The neurofibromatoses: a pathogenetic and clinical overview. Chapman and Hall Medical, London, pp 160–232

Jenne DE, Tinschert S, Stegmann E, Reimann H, Nuernberg P, Horn D, Naumann I, Buske A, Thiel G (2000) A common set of at least 11 functional genes is lost in the majority of NF1 patients with gross deletions. Genomics 66:93–97

Ji Y, Eichler EE, Schwartz S, Nicholls RD (2000) Structure of chromosomal duplicons and their role in mediating human genomic disorders. Genome Res 10:597–610

Kayes LM, Riccardi VM, Burke W, Bennett RL, Stephens K (1992) Large de novo DNA deletion in a patient with sporadic neurofibromatosis 1, mental retardation, and dysmorphism. J Med Genet 29:686–690

Kayes LM, Burke W, Riccardi VM, Bennett R, Ehrlich P, Rubenstein A, Stephens K (1994) Deletions spanning the neurofibromatosis 1 gene: identification and phenotype of five patients. Am J Hum Genet 54:424–436

Kehrer-Sawatzki H, Haeussler J, Krone W, Bode H, Jenne DE, Mehnert KU, Tuemmers U, Assum G (1997) The second case of a t(17;22) in a family with neurofibromatosis type 1: sequence analysis of the breakpoint regions. Hum Genet 99:237–247

Kiyosawa H, Lensch MW, Chance PF (1995) Analysis of the CMT1A-REP repeat: mapping crossover breakpoints in CMT1A and HNPP. Hum Mol Genet 4:2327–2334

Kumar S, Hedges SB (1998) A molecular timescale for vertebrate evolution. Nature 392:917–920

Lander ES, Linton LM, Birren B, Nusbaum C, Zody MC, Baldwin J, Devon K et al. (2001) Initial sequencing and analysis of the human genome. Nature 409:860–921

Lazaro C, Gaona A, Ainsworth P, Tenconi R, Vidaud D, Kruyer H, Ars E, Volpini V, Estivill X (1996) Sex differences in mutational rate and mutational mechanism in the NF1 gene in neurofibromatosis type 1 patients. Hum Genet 98: 696–699

Leppig KA, Viskochil D, Neil S, Rubenstein A, Johnson VP, Zhu XL, Brothman AR, Stephens K (1996) The detection of contiguous gene deletions at the neurofibromatosis 1 locus with fluorescence in situ hybridization. Cytogenet Cell Genet 72:95–98

Leppig K, Kaplan P, Viskochil D, Weaver M, Orterberg J, Stephens K (1997) Familial neurofibromatosis 1 gene deletions: cosegregation with distinctive facial features and early onset of cutaneous neurofibromas. Am J Med Genet 73: 197–204

Lopes J, Ravise N, Vandenberghe A, Palau F, Ionasescu V, Mayer M, Levy N, Wood N, Tachi N, Bouche P, Latour P, Ruberg M, Brice A, LeGuern E (1998) Fine mapping of de novo CMT1A and HNPP rearrangements within CMT1A-REPs evidences two distinct sex-dependent mechanisms and candidate sequences involved in recombination. Hum Mol Genet 7:141–148

Lopes J, Tardieu S, Silander K, Blair I, Vandenberghe A, Palau F, Ruberg M, Brice A, LeGuern E (1999) Homologous DNA exchanges in humans can be explained by the yeast double-strand break repair model: a study of 17p11.2 rearrangements associated with CMT1A and HNPP. Hum Mol Genet 8:2285–2292

Lopez-Correa C, Brems H, Lazaro C, Estivill X, Clementi M, Mason S, Rutkowski JL, Marynen P, Legius E (1999) Molecular studies in 20 submicroscopic neurofibromatosis type 1 gene deletions. Hum Mutat 14:387–393

Lopez-Correa C, Brems H, Lazaro C, Marynen P, Legius E (2000) Unequal meiotic crossover: a frequent cause of NF1 microdeletions. Am J Hum Genet 66:1969–1974

Lupski JR (1998) Genomic disorders: structural features of the genome can lead to DNA rearrangements and human disease traits. Trends Genet 14:417–422

Messiaen LM, Callens T, Mortier G, Beysen D, Vandenbroucke I, Van Roy N, Speleman F, Paepe AD (2000) Exhaustive mutation analysis of the NF1 gene allows identification of 95% of mutations and reveals a high frequency of unusual splicing defects. Hum Mutat 15:541–555

Pentao L, Wise CA, Chinault AC, Patel PI, Lupski JR (1992) Charcot-Marie-tooth type 1A duplication appears to arise from recombination at repeat sequences flanking the 1.5 Mb monomer unit. Nat Genet 2:292–300

Rasmussen SA, Colman SD, Ho VT, Abernathy CR, Arn PH, Weiss L, Schwartz C, Saul RA, Wallace MR (1998) Constitutional and mosaic large NF1 gene deletions in neurofibromatosis type 1. J Med Genet 35:468–471

Reiter LT, Murakami T, Koeuth T, Gibbs RA, Lupski JR (1997) The human COX10 gene is disrupted during homologous recombination between the 24 kb proximal and distal CMT1A-REPs. Hum Mol Genet 6:1595–1603

Reiter LT, Hastings PJ, Nelis E, De Jonghe P, Van Broeckhoven C, Lupski JR (1998) Human meiotic recombination products revealed by sequencing a hotspot for homologous strand exchange in multiple HNPP deletion patients. Am J Hum Genet 62:1023–1033

Riva P, Castorina P, Manoukian S, Dalpra L, Doneda L, Marini G, den Dunnen J, Larizza L (1996) Characterization of a cytogenetic 17q11.2 deletion in an NF1 patient with a contiguous gene syndrome. Hum Genet 98:646–650

Riva P, Corrado L, Natacci F, Castorina P, Wu BL, Schneider GH, Clementi M, Tenconi R, Korf BR, Larizza L (2000) NF1 microdeletion syndrome: refined FISH characterization of sporadic and familial deletions with locus-specific probes. Am J Hum Genet 66:100–109

Side LE, Shannon KM (1998) The NF1 gene as a tumour suppressor. In: Upadhyaya M and Cooper DN (eds), Neurofibromatosis type 1, from genotype to phenotype. Bios Scientific, Oxford, pp 133–146

Tinschert S, Naumann I, Stegmann E, Buske A, Kaufmann D, Thiel G, Jenne DE (2000) Segmental neurofibromatosis is caused by somatic mutation of the neurofibromatosis type 1 (NF1) gene. Eur J Hum Genet 8:455–459

Tonsgard JH, Yelavarthi KK, Cushner S, Short MP, Lindgren V (1997) Do NF1 gene deletions result in a characteristic phenotype? Am J Med Genet 73:80–86

Upadhyaya M, Ruggieri M, Maynard J, Osborn M, Hartog C, Mudd S, Penttinen M, Cordeiro I, Ponder M, Ponder BA, Krawczak M, Cooper DN (1998) Gross deletions of the neurofibromatosis type 1 (NF1) gene are predominantly of maternal origin and commonly associated with a learning disability, dysmorphic features and developmental delay. Hum Genet 102:591–597

Venter JC, Adams MD, Myers EW, Li PW, Mural RJ, Sutton GG, Smith HO, et al. (2001) The sequence of the human genome. Science 291:1304–1351

Wu B-L, Austin M, Schneider G, Boles R, Korf B (1995) Deletion of the entire NF1 gene detected by FISH: four deletion patients associated with severe manifestations. Am J Med Genet 59:528–535

Yunis JJ, Prakash O (1982) The origin of man: a chromosomal pictorial legacy. Science 215:1525–1530